# Mitonuclear interactions impact aerobic metabolism in hybrids and may explain mitonuclear discordance in young, naturally hybridizing bird lineages

Authors: Callum S. McDiarmid[1*], Daniel M. Hooper[2], Antoine Stier[3,4], Simon C. Griffith[1]

[1] School of Natural Sciences, Macquarie University, Sydney, NSW, Australia; [2] Institute for Comparative Genomics, American Museum of Natural History, New York, NY, USA; [3] Department of Biology, University of Turku, Turku, Finland; [4] Institut Pluridisciplinaire Hubert Curien, UMR7178, Université de Strasbourg, CNRS, Strasbourg, France

*correspondence: callum.mcdiarmid@students.mq.edu.au

Keywords: speciation, introgression, mitonuclear, mitochondrial, aerobic respiration, hybridization, cyto-nuclear discordance

## Abstract

Understanding genetic incompatibilities and genetic introgression between incipient species are major goals in evolutionary biology. Mitochondrial genes evolve rapidly and exist in dense gene networks with coevolved nuclear genes, suggesting that mitochondrial respiration may be particularly susceptible to disruption in hybrid organisms. Mitonuclear interactions have been demonstrated to contribute to hybrid disfunction between deeply divergent taxa crossed in the laboratory, but there are few empirical examples of mitonuclear interactions between younger lineages that naturally hybridise. Here we use experimental crosses and high resolution respirometry to provide the first evidence in a bird that inter-lineage mitonuclear interactions impact mitochondrial aerobic metabolism. Specifically, respiration capacity of the two paternal backcrosses (with mismatched mito-nuclear combinations) differ from one another, although they do not differ to the parental groups or maternal backcrosses as we would expect of mitonuclear disruptions. In the wild hybrid zone between these subspecies the mitochondrial cline centre is shifted west of the nuclear cline centre, which is consistent with the direction of our experimental results. Our results therefore demonstrate asymmetric mitonuclear interactions that impact the capacity of cellular mitochondrial respiration and may help to explain the geographic discordance between mitochondrial and nuclear genomes in the wild.

## Introduction

Understanding the factors that obstruct gene flow or propel genetic introgression between biological lineages is a central goal of speciation research[1]. One factor that may be particularly susceptible to disruption in hybrids is the interaction between the mitochondrial and nuclear genomes, which underpin mitochondrial aerobic metabolism[2–4]. Functional mitochondria rely on dense gene networks encompassing genes in both the mitochondrial (N = ~37 genes) and nuclear (N = ~1,500 genes) genomes (Fig. 1A)[5–7], and these genes (particularly mitochondrial genes) can undergo rapid synonymous change between lineages [8–12]. Following hybridization, novel combinations of mtDNA and nuDNA may disrupt mitochondrial function and thus act as a barrier to gene flow.

Inter-lineage mitonuclear interactions – i.e., interactions between the mitochondria of one lineage and the nuclear genome of another lineage that occur within the cells of hybrids - have been demonstrated to contribute to hybrid disfunction between deeply divergent taxa crossed in the laboratory [13–17]. There are, however, fewer empirical examples of inter-lineage mitonuclear interactions between younger taxa that naturally hybridise [18–20]. In birds, there is suggestive evidence from hybrid zones that mitonuclear incompatibilities may contribute to reproductive isolation [21–23]. Direct evidence linking hybrid disfunction with mitonuclear incompatibilities is lacking, however, in large part because most birds cannot be readily kept and bred in captivity. This precludes controlled experiments to effectively disassociate the mitochondrial and nuclear genomes. Naturally produced hybrids that have low physiological function may be compromised for various other reasons, such as their parents mating with a heterospecific because they were poor quality individuals [24]. In contrast to genetic incompatibilities of uniform effect on hybrid fitness, interactions of asymmetrical effect [i.e., differential fitness between hybrids based on direction of cross] can result in certain genes introgressing beyond the hybrid zone, resulting in geographic discordance between different regions of the genome. In naturally hybridizing systems, geographic discordance between mtDNA and nuDNA is observed at an appreciable frequency but the underlying mechanisms are rarely understood[25]. Discordance is often attributed to demographic disparities or sex-biased asymmetries based mostly on verbal arguments[26], while the functional consequences of mitonuclear interactions such as those described here are rarely considered [25,27,28].

Optimal function of mitochondrial respiration in birds is dependent on 37 genes in the mtDNA, including 13 protein coding genes that encode key components of the well charactersied complexes I, III, IV and V in the electron transport system (ETS) on the inner mitochondrial membrane. In addition,

the avian mtDNA encodes two ribosomal RNAs (rRNAs), 22 transfer RNAs (tRNAs) and a control region (OH). Disfunction of these mitochondrial genes can impact fitness in humans and is illustrative of what might be expected from inter-lineage mitonuclear incompatibilities. Mutations in human mtDNA, for example, can manifest as mitochondrial diseases and are associated with disorders such as neurodegeneration[29,30]. Changes in the amino acid composition of ETS subunits, or genetic substitutions in the tRNA or rRNA machinery that impact the transcription or translation of ETS subunits, can both potentially destabilise the transfer of high-energy electrons causing them to leak from the ETS. Leaking electrons can contribute to the formation of reactive oxygen species (ROS) that can damage cellular macromolecules[30].

The subspecies of the long-tailed finch *Poephila acuticauda acuticauda* and *P. a. hecki* inhabit tropical savannahs across northern Australia and naturally hybridise where their distributions meet on the edge of the Kimberley Plateau in Western Australia[31]. Previous work has estimated they last shared a common ancestor approximately 0.5 million years ago (0.31 – 0.68 Mya, 95% HPD) based on divergence in three mtDNA genes[32]. Mitonuclear discordance has been observed in the wild hybrid zone between these two subspecies, with the centre of the mitochondrial cline being 55 km west of the nuclear cline centre[32], but within the boundaries of the nuclear hybrid zone (Fig. 1B & C, [32]). This discordance suggests the eastern mitochondrial lineage (mitotype) has introgressed westward across the hybrid zone. One possible explanation for this apparent introgression is that hybridisation causes novel mitonuclear interactions that asymmetrically reduce the fitness of individuals with a western mitotype and eastern nuclear genome, by adversely impacting aerobic metabolism and therefore ATP synthesis, or through elevated generation of reactive oxygen species (ROS) that results in oxidative stress. The long-tailed finch can be readily kept and bred in captivity, making it an experimentally tractable model system in which to examine the consequences of this potential mitonuclear mismatch.

In this study we use subspecies of the long-tailed finch to test whether inter-lineage mitonuclear interactions impact aerobic metabolism. We used wild-derived captive long-tailed finches to create particular crosses that should expose any inter-lineage mitonuclear interactions that exist between the subspecies in the resulting embryos. We then assessed mitochondrial aerobic respiration capacity using high-resolution respirometry[33] of these embryos.

## Methods

## Study species

This project used long-tailed finches of each subspecies (*Poephila acuticauda acuticauda* and *P. a. hecki*) that were part of the captive population maintained at Macquarie University in Sydney, Australia. Wild caught *P. a. acuticauda* individuals were originally sourced from Mount House (17°02'S, 125°35'E) and Nelson's Hole (15°49'S, 127°30'E) in Western Australia, and wild-caught *P. a. hecki* were sourced from October Creek (16°37'S, 134°51'E) in the Northern Territory[34,35].

In this experiment we compared measures of cellular respiration (Oroboros $O_2K$); a proxy for embryo metabolism (heart rate); and a proxy for oxidative damage, among groups in which the lineage of the mitochondrial genotype (mitotype) either matched or did not match the lineage of the nuclear genome. Working with embryos meant we eliminated the opportunity for the effects of extended parental care by parents of different genotype/mitotype. In our experiment there was no significant difference between experimental groups in embryonic survival ($X^2_5 = 4.1$, $p = 0.53$; Fig. S3B) or mass at day 12 of incubation ($X^2_5 = 7.3$, $p = 0.20$; Table 3; Fig. S3C).

### Breeding

Embryos were produced by rotating pairs of long-tailed finches through 20 outdoor aviaries (4.1 m long x 1.85 m wide x 2.24 m high), with one pair per aviary containing three nesting boxes and nesting material. Mealworms, greens, dry seed, and water were provided *ad libitum*. We required females to have been exclusively with the partner for 14 days minimum before any experimental eggs were collected, to avoid embryos being sired by stored sperm from a different male – any eggs laid before 14 days were collected and destroyed on the day of lay. Nest boxes were checked every day, and eggs were collected the day they were laid, given a unique number using a felt-tipped permanent marker, and stored in a 'soft box' at cool room temperature (22 °C) for up to seven days before being placed into an incubator (Brinsea Ovation 56 EX, Brinsea Products, Winscombe, U.K.). Eggs were incubated at 37.5°C and 65% humidity for 12 days. On the 12$^{th}$ day (i.e., the day before expected hatch) eggs were removed and measurements made.

## Crossing

We produced backcrossed offspring by breeding $F_1$ hybrid females with an unadmixed 'pure' male of each subspecies, sequentially and in random order. The resulting offspring were maternal backcrosses if their father's lineage *did* match their mother's mitotype and were paternal backcrosses if father's lineage *did not* match their mother's mitotype (Fig. 3A). Pure parental pairs of each subspecies were set up to breed at the same time and used as controls.

135 Paternal backcrossing exposes incompatibilities by producing offspring who inherit most of
136 their nuclear genome from a different lineage to that of their mitochondrial genome (Fig. 3A). This is
137 particularly pronounced in the case of the long-tailed finch, as >98.5% of fixed nuclear differences
138 between subspecies are on the Z-chromosome[36]. In our cross design, paternal backcross offspring
139 inherit Z chromosomes that have had no opportunity for recombination between subspecies. If male,
140 they receive one Z chromosome from their hemizygous $F_1$ mother and a matching Z chromosome of
141 the same subspecies from their 'pure' father. Females have only a single Z chromosome inherited from
142 their father. Paternal backcrosses have mismatched mitochondrial and nuclear genomes, but also
143 have a low level of admixture on autosomes in their nuclear genome, which would otherwise be a
144 potentially confounding source of hybrid disfunction. For this reason, we included maternal backcross
145 (MB) individuals as controls, as their level of autosomal admixture is the same as paternal backcrosses,
146 but their mitochondria and Z chromosomes are from the same lineage. We also included pure-
147 breeding (parental) individuals of each subspecies as further control groups. It is worth noting that
148 these several different types of backcrossed hybrids are also highly relevant to the wild hybrid zone,
149 where we previously described that ~68% (243 of 357) of individuals had some level of admixture[32].
150
151 The goal of this cross design was to create embryos in which the mitochondrial genotype
152 (mitotype) of each subspecies (*P. a. acuticauda and hecki*) was placed in three contexts: 1) a nuclear
153 genetic background exactly matching the mitotype lineage (parental cross), 2) a nuclear genetic
154 background that mostly did not match the mitotype lineage (paternal backcross) and 3) a nuclear
155 genetic background that mostly did match the mitotype lineage (maternal backcross). The six groups
156 of embryos were thus 1. parental *hecki* (*hecki* mother, *hecki* father), 2. Paternal backcross *hecki*
157 mtDNA ($F_1$ mother with *hecki* mtDNA, *acuticauda* father), 3. Maternal backcross *hecki* mtDNA ($F_1$
158 mother with *hecki* mitotype, *hecki* father), 4. parental *acuticauda* (*acuticauda* mother, *acuticauda*
159 father), 5. Paternal backcross *acuticauda* ($F_1$ mother with *acuticauda* mtDNA, *hecki* father) and 6.
160 Maternal backcross yellow ($F_1$ mother with *acuticauda* mtDNA, *acuticauda* father). $F_1$ hybrid females
161 themselves had one *acuticauda* and one *hecki* parent. All male parents were only used once and were
162 either 'pure' *acuticauda* or 'pure' *hecki*. For females, 'pure' *acuticauda* and 'pure' *hecki* were only used
163 for one clutch each. First generation ($F_1$) hybrid females were typically used for two clutches, one with
164 a *hecki* male partner and one with an *acuticauda* male partner (although N = 4 $F_1$ females only
165 produced a clutch with one partner).
166
167 **Heart rate measurement**

168 After 12 days of incubation each embryo was removed from the incubator, and immediately placed
169 on a Buddy digital egg monitor (Vetronic Services, Abbotskerswell, Devon, U.K.), that gives a digital
170 readout of embryonic heart rate from within the egg (a proxy for whole body metabolic rate)[37]. A
171 timer was started when the egg was removed from the incubator, and heart rate and corresponding
172 time since removal were recorded at least twice over 2 minutes, but as many times as possible. The
173 lower temperature outside the incubator meant that embryonic heart rate decreased over those two
174 minutes, but we used the several measurements to calculate the rate of cooling and the predicted
175 heart rate halfway through the period (i.e., at 60 seconds). The five individuals where heart rate was
176 only measured once were excluded from this dataset.
177

178 **High resolution respirometry strategy**

179 High resolution respirometry was performed with permeabilised tissue samples from these embryos
180 using an Oroboros O2k (Oroboros Instruments, Innsbruck, Austria). High resolution respirometry
181 allowed us to systematically stimulate, uncouple and inhibit certain combinations of mitochondrial
182 complexes (Table 3; Fig. S1). We measured the maximum capacity of OXPHOS system when fuelled by
183 electrons either through both complex I, or both I and II in tandem (OXP-I, OXP-I,II), and the maximum
184 capacity of the ETS when accepting electrons from CxII, and both CxI and II in tandem (ETS-I,II, ETS,II).
185 Comparing our experimental groups for these measures reveals whether CxI is compromised. We also
186 assessed the maximum capacity for complex IV in isolation to consume $O_2$, a measure not reliant on
187 CxIII, which can reveal if CxIII is compromised. We assessed LEAK-I,II respiration, which reflects
188 respiration not available to fuel ATP synthesis. These measures hence allow us to test whether there
189 is an impact of mitonuclear interactions on mitochondrial aerobic metabolism, and to dissect whether
190 either complex with amino acid differences between subspecies is likely involved (CxI and III), or
191 whether it is more likely a translational issue related to fixed differences in the mtDNA encoded tRNAs
192 or rRNAs. It is possible that some aspect of mitochondrial function other than aerobic respiration is
193 impaired but that respiration rate is maintained and for that reason we also measured ROS-induced
194 damage. High ROS levels resulting from mitochondrial disfunction can damage macromolecules, cell
195 components and structures[38,39] and ROS-induced DNA damage correlates with shorter lifespan in
196 the closely related zebra finch[40].
197

198 **High resolution respirometry technical steps**

199 After the embryonic heart rate was measured, embryos were used for high resolution respirometry.
200 Embryos were euthanised via decapitation and then weighed (Mettler Toledo, PB303-S/FACT,
201 Colombus, Ohio, USA). The head and body were then laterally cut into two, and the right-hand side

202 was placed in 400 µl of phosphate buffered saline (PBS) and then homogenized with three strokes of
203 a teflon-glass Potter-Elvehjem homogenizer (Wheaton, 5 mL) and stored at -80 for later analyses
204 including DNA extraction for sex determination (described below). The left-hand side was then
205 weighed, and diluted 100 mg/mL of MiR05 medium (0.5 mM Egtazic Acid (EGTA), 3 mM MgCl2, 50
206 mM K-lactobionate, 20 mM taurine, 10 mM KH2PO4, 20 mM Hepes, 110 mM sucrose, free fatty acid
207 bovine serum albumin (1 g L-1), pH 7.1;[41,42]), and then homogenized and mechanically
208 permeabilised using a teflon-glass Potter-Elvehjem homogenizer (Wheaton, 5 mL). All work was done
209 on ice. This homogenate was then centrifuged for 1 min at 100 g to pellet big tissue, and then 500ul
210 of the supernatant was added to a chamber of an $O_2$k high resolution respirometer set at 37°C. After
211 both samples were loaded and the system had equilibrated (oxygen consumption was stable), 2 µl of
212 digitonin (10 mg/mL) was added to ensure cells were fully permeabilised. We injected 5 µl pyruvate
213 (5mM final), 5 µl malate (2mM final), 10 µl glutamate (10mM final) as electron donors for complex I.,
214 and then measured oxidative phosphorylation when only complex I was receiving electrons (OXPHOS-
215 I) by adding 5 µl adenosine diphosphate (ADP, 1.25 mM final). We next measured coupled respiration
216 capacity through both complexes I and II (OXPHOS-I,II) by adding 25 µl succinate (10 mM final). We
217 then determined $O_2$ consumption associated with proton leak when electrons were being received by
218 both complex I and II (LEAK-I,II) by adding 5 µl oligomycin (10 uM final). We next estimated the
219 maximum capacity of the electron transport system (ETS-I,II) by titrating the mitochondrial uncoupler
220 carbonyl cyanide m-chlorophenyl hydrazine (CCCP; at 2 mM concentration) by first one injection of 3
221 µl, followed by 1 µl steps. We next estimated the ETS capacity when only receiving electrons through
222 complex II (ETS-II) by adding 1 µl rotenone (0.5 uM final). We then measured non-mitochondrial O2
223 consumption by injecting 1 µl of antimycin A (2.5 uM final) to inhibit complex III. Finally, we estimated
224 the respiration capacity of complex IV directly (CxIV) by first adding 5 µl TMPD (0.5 mM final) and 5 µl
225 ascorbate (2 mM final), and then calculating the background chemical respiration rate by adding 50 µl
226 azide (100 mM final). Across all runs the chambers were opened consistently at the same stages for
227 reoxygenation. After each run 1 ml of the solution was taken from each Oroboros chamber and frozen
228 at -80 °C, and at the conclusion of all measures we performed a Pierce BCA protein quantification
229 assay on this stored solution (ThermoFisher, Scientific, Waltham, MA, USA). Protein quantity was
230 included as a covariate in statistical models (below) to account for slight differences in the amount of
231 biological material in each sample. In most cases a different embryo sample was run in each chamber,
232 but in 40 cases the same embryo was run in duplicate to assess how repeatable these measurements
233 were (Table 3). When two different samples were run, the first was sitting in the Oroboros for some
234 time before the protocol was begun, and to account for any variability introduced by this we included

235 a covariate in our models that was the length of time between when the embryo sample entered the
236 chamber and when the measure was made.
237
238 **Molecular sexing**
239 We extracted DNA from the homogenized right- side of all embryos using a Gentra PureGene kit
240 (Qiagen, Valencia, CA, USA) following manufacturer's instructions. We sexed embryos by amplifying
241 an intronic portion of the CHD gene that differs in size between the Z-linked and W-linked copy
242 following published protocols[32,43]. Gel electrophoresis of the PCR product revealed the sex of the
243 embryo as either male (one band, homozygous, ZZ) or female (two bands, heterozygous, ZW).
244
245 **mtDNA copy number**
246 We estimated mitochondrial density for all samples using real-time quantitative PCR (qPCR) analysis
247 following protocols established for other passerine birds (Stier et al. 2019, 2022), generating data for
248 215 individuals. This provides mtDNA copy number which only provides a proxy of mitochondrial
249 density, since the amount of mtDNA in a mitochondria can vary. We estimated the relative mtDNA
250 copy number by measuring the amount of mtDNA relative to the nuDNA for each sample by qPCR on
251 a CFX96 Real-Time System (BIO-RAD). We used RAG1 as a representative single-copy nuclear gene (F:
252 GCAGATGAACTGGAGGCTATAA, R: CAGCTGAGAAACGTGTTGATTC). We confirmed that there is only a
253 single copy of RAG1 in the long-tailed finch by examining the relative depth of coverage for RAG1
254 against mean depth for the entirety of chromosome 5 for five individuals of each subspecies, mapped
255 to the zebra finch reference genome (GCA_003957565.4), which only has a single RAG1 copy. There
256 was no difference in depth between RAG1 and chromosome 5, with mean ratio of RAG1:chr5 being
257 1.04 (if there were two copies the expectation would be a ratio of ~2). For our mitochondrial gene we
258 used COX1 (F: TCCTAGCCAACTCCTCAC, R: CCTGCTAGGATTGCAAAT). We observed a complete nuclear
259 copy of the mitochondrial genome (i.e., NUMT) in Estrildid finches; for example, in the zebra finch
260 reference genome (GCA_003957565.4: chr2:72232845-72249691). As avian blood has a much higher
261 nuclear:mitochondria ratio than muscle, DNA extracted from blood is much more likely to result in
262 amplification of the NUMT than DNA extracted from muscle[44]. As such we designed primers without
263 ambiguous sites to perfectly match the mitochondrial sequence observed as conserved in *Poephila*
264 and not the apparent pseudo-gene in the nuclear genome (Daniel Hooper, unpublished data) by
265 basing the primer off DNA extracted from muscle tissue. We verified that they resulted in one single
266 product of the expected size on agarose gel.
267

268 Following Stier et al. (2022), qPCR reactions had a total volume of 12 µl that included 6 ng of
269 DNA, had PCR primers with concentrations of 200 nM and 6 µl of Absolute Blue qPCR Mix SYBR Green
270 low ROX (Thermos Scientific). The qPCR conditions were: 15 mins at 95°C, 40 cycles of 15 s at 95°C, 30
271 s at 58°C, 30 s at 72°C. Samples were run in triplicate for each gene (RAG1 and COX1) across 5 plates,
272 ten samples were pooled and included on every plate as a reference, and 20 samples were included
273 on two separate plates. Amplicon efficiency was estimated from a standard curve of the reference
274 between 1.5 to 24 ng (1.5, 3, 6, 12, 16, 24) run on one plate. The mean reaction efficiencies were
275 92.1% for RAG1 and 82.3% for COX1. To calculate relative mtDNA copy number for each sample we
276 used the following formula: $(1+Ef_{COX1})^{\Delta CqCOX1}/(1+Ef_{RAG1})^{\Delta CqRAG1}$, with Ef as the amplicon efficiency, ΔCq
277 as the difference in Cq between the reference and focal samples. Some samples were run twice on
278 separate plates, with an inter-plate repeatability of 0.74 (95% C.I. [0.49, 0.88]), and based on triplicates
279 intra-plate repeatability was 0.94 (95% C.I. [0.93, 0.95]). Seven samples were considered as outliers
280 (Cq RAG1 < Cq COI) and removed from analysis.
281
282 **Oxidative Damage assay**
283 8-OHdG (8-hydroxy-2'-deoxyguanosine) is a predominant form of ROS-induced oxidative lesion that
284 has been widely used as a biomarker for oxidative damage[45], including alongside measures of
285 respiration capacity in birds[46,47]. Here we quantified levels of 8-OHdG in the DNA extracted from
286 embryos using a competitive immunoassay (300 ng DNA, EpiQuick 8-OHdG DNA Damage
287 Quantification Direct Kit Colorimetric, Epigentek, USA) following the manufacturer recommendations.
288 This was run on a subset of samples (N = 182) chosen blind to respiration capacity to have roughly
289 balanced numbers from each experimental group (N = 28-33 samples per group). The intra-plate
290 coefficient of variation based on duplicates was 6.3 ± 0.83. The inter-plate coefficient of variation
291 based on four samples repeated over all three plates was 22.7 ± 4.05, so we included plate ID as
292 random effect in our analyses.
293
294 **mtDNA comparison between subspecies**
295 Changes in the mitochondrial genome are required but not sufficient for inter-lineage mitonuclear
296 incompatibility. Even a single substitution in the mtDNA can lead to reproductive isolation (e.g.,
297 [48]). To identify substitutions with the potential to contribute to incompatibilities, we sequenced
298 whole mitochondrial genomes from each long-tailed finch subspecies and counted the number of
299 fixed differences and associated amino acid changes within 13 protein coding genes between them.
300 We assembled mitochondrial genomes using whole genome sequence (WGS) data, generated for a
301 pending study now in prep, from both long-tailed finch subspecies (*P. a. acuticauda,* N = 14; *P. a.*

302 *hecki* N = 11) and their sister species the black-throated finch (*P. cincta atropygialis* N = 11) using
303 bcftools (version 1.9)[49] consensus after calling and incorporating variants relative to the zebra
304 finch reference genome (GCF_003957565.2) in each sample. Ambiguous positions were output with
305 associated IUPAC codes[43]. We exclusively used WGS data derived from DNA extracted from
306 muscle (rather than blood) to ensure that they were enriched for reads from mitochondrial DNA and
307 not reads from the nuclear encoded mtDNA (NUMT) copy. The mitochondrial genome of the zebra
308 finch reference (bTaeGut1.4pri) was used as an additional outgroup to help assign substitutions to
309 their lineage of origin. We used the MITOS2 WebServer[50] to extract specific sequences for each
310 mtDNA encoded gene, including all 13 protein coding genes, 22 tRNA and 2 rRNA and the control
311 region. Each gene was aligned using MAFFT (version 7) web-aligner[51] and we manually examined
312 each alignment with Geneious prime (version 2023.1.2) to count and characterize the distribution of
313 fixed differences between each of the three members of *Poephila* (Table S1). For each protein-
314 coding gene, we used the number of fixed differences between subspecies to quantify their absolute
315 divergence ($D_{XY}$).
316
317 We next evaluated the extent of non-synonymous change between long-tailed finch
318 subspecies for each protein-coding gene. We generated lineage-specific consensus sequences for
319 each gene and used the vertebrate mitochondrial genetic code to translate these to amino acid
320 sequence We again used data from the black-throated finch and zebra finch as outgroups to assign
321 amino acid changes to the long-tailed finch subspecies of origin. We classified each amino acid
322 substitution by any associated change in biochemical properties. Finally, we calculated the ratio of the
323 rate of non-synonymous to the rate of synonymous nucleotide substitutions (dN/dS) between long-
324 tailed finch subspecies for each protein-coding gene using the model M0 implemented in the program
325 Easy-CodeML (v1.41)[52].
326
327 **Statistics**
328 For statistical analyses we used R version 4.1.2 (R Core Team 2020) using RStudio version 1.2.5033
329 (RStudio Team, 2020) for the graphical interface. We used the lme4 and lmerTest packages[53,54] to
330 run linear mixed models to test whether our measures of respiration capacity differed between the
331 six experimental groups ('pure' acuticauda, 'pure' hecki, paternal and maternal backcross with
332 acuticauda mtDNA, paternal and maternal backcrosses with hecki mtDNA). These measures were each
333 included as the dependent variable in separate linear mixed models, in which the fixed effects were
334 experimental group, embryo sex, protein quantity in the chamber, and the length of time after embryo
335 entered the oroboros chamber when the measure was made. In each we tested for an interaction

336 between experimental group and embryo sex, and if this was not significant the interaction term was
337 removed (but left in the model if significant). In each model parental pair ID was included as a random
338 effect, to account for multiple members of the same clutch being included. Where there was a
339 significant effect of experimental group, we ran Tukey post-hoc comparisons using the emmeans
340 package[55] to assess specifically which groups differed from one another. Model assumptions were
341 checked using the DHARMa package in R[56].
342
343 We similarly ran linear mixed models to test whether heart rate, oxidative damage and
344 mitochondrial copy number differed between our experimental groups, but in these cases the fixed
345 effects were experimental group, embryo sex, and for the heart rate model embryo mass, and the
346 random effect was still parental pair ID. Oxidative damage and mitochondrial copy number were log-
347 transformed to better meet model assumptions. An interaction between experimental group and sex
348 was also included for each model, but then removed if not significant. In the mitochondrial copy
349 number and oxidative damage models, plate ID were additionally included as random effects. Embryo
350 ID was also initially included as a random effect in the mitochondrial copy number and oxidative
351 damage models, but it explained close to zero variance so was removed for the final models, likely
352 because very few individuals were measured twice (10 for mt copy number, 21 for oxidative damage).
353 A small number of values for mitochondrial copy number were extremely high (N = 10, total N = 211),
354 well above the normally distributed other samples and were likely technical errors, and so were
355 excluded to facilitate modelling. When plotted they were distributed roughly evenly between
356 experimental groups so their inclusion would be unlikely to change the results anyway.
357

358 ## Results

359
360 We found a low level of divergence in mtDNA between subspecies, with fixed differences observed in
361 only 0.9% of positions comprising the protein-coding genes of the electron transport system (107 of
362 11,361 bp total; Table 1). Absolute divergence ($D_{XY}$) was highly variable, however, across protein-
363 coding genes, ranging from 0% (ATP8) to 3.3% (NAD6), and between complexes: divergence was 2.1-
364 fold higher on average for genes in complex I than in complex IV (Table 1). We observed a total of
365 seven fixed amino acid differences between subspecies, five differences in four genes in complex I,
366 and two amino acid differences in the cytochrome b (COB) gene in complex III. There were no amino
367 acid differences between the subspecies in either complex IV or complex V. The inferred mitochondrial
368 genome-wide dN/dS ratio between long-tailed finch subspecies is well below 1 at 0.0168, suggesting
369 that purifying selection is the dominant force shaping mitochondrial evolution in *Poephila* (Table 1).

370 Of the five genes with observed non-synonymous differences between subspecies, dN/dS ranged from
371 0.0127 (*NAD5*) to 0.1142 (*NAD3*).
372
373 In the non-coding region, we observed a further six fixed differences between subspecies in
374 the small and large rRNA genes (four and two differences, respectively) and a total of four fixed
375 differences in four mitochondrial tRNAs (Table S1). These non-coding differences provide additional
376 potential sites of mitonuclear incompatibilities that could impact mitochondrial function via the
377 transcription, translation, or replication of mtDNA [e.g., 41]. On the other hand, any protein-protein
378 mitonuclear incompatibilities in this system should be restricted to impacting the function of
379 complexes I or III.
380
381 Polarization inference from the use of outgroup taxa revealed that of the seven fixed amino
382 acid differences between subspecies, six have occurred in the *hecki* lineage (Table 2; Fig. 2). Three of
383 the amino acid substitutions derived within *hecki*, and the single amino acid change derived in
384 *acuticauda*, result in a change from a polar to a non-polar amino acid (Table 2). In the non-protein
385 coding genes (rRNAs, tRNAs, OH) there was a roughly even spread of derived DNA sequence changes
386 between lineages (6 *acuticauda* and 4 *hecki,* Table S1; Table S3).
387
388 There was a significant difference between the two paternal backcross groups for all five
389 measures of aerobic respiration capacity (except borderline non-significant for females for OXP-I,II, p
390 = 0.064), whereby individuals with *acuticauda* mtDNA and *hecki* nuDNA had lower respiration capacity
391 than did individuals with *hecki* mtDNA and *acuticauda* nuDNA (Table 3; Fig. 3, Fig. S2). There were no
392 other differences between experimental groups that were as consistent across the five measures of
393 aerobic capacity we measured (Table 3). For the measure ETS-I,II the paternal backcross *hecki*
394 mitotype was significantly higher than the maternal backcross *acuticauda* mitotype, and for OXP-I
395 females the parental group *hecki* was significantly higher than the paternal backcross *acuticauda*
396 mitotype group (Table 3).
397
398 We did not find a difference between groups in oxidative damage (Table 3, Fig. S3D). We also
399 found no evidence that this difference in aerobic respiration capacity between paternal backcross
400 groups was driven by different quantities of mitochondria per cell, with the relative mtDNA copy
401 number not significantly differing between the two paternal backcross groups, or between them and
402 other groups (Table 3) and so likely not driving the aerobic respiration capacity results. Our proxy for
403 whole-organism metabolic rate was heart rate on day 12 of incubation immediately after being

404 removed from the incubator, for which we found no difference between experimental groups, so no
405 evidence that whole body metabolism is impacted (Table 2, Fig. S3C).
406

407 ## Discussion

408

409 We found evidence that an interaction between the mitochondrial and nuclear genomes of the long-
410 tailed finch subspecies impacted aerobic respiration capacity, despite the low level of divergence in
411 mtDNA between them (<1%). These observations identifying the effect of mitonuclear
412 incompatibilities on aerobic respiration have important implications for both mtDNA introgression
413 and reproductive isolation in the long-tailed finch system. Positive selection can drive allelic
414 introgression across a hybrid zone, as can neutral processes (such as range expansion). In the long-
415 tailed finch hybrid zone there are high levels of admixture (~68% of individuals have some degree of
416 mitonuclear mismatch), and so selection will be acting on each mitotype in several different nuclear
417 contexts, similar to those generated through our experimental approach. Our primary result
418 suggests that there is no difference in mitochondrial aerobic metabolism between the mitotypes in
419 the pure parental context or in the maternal backcross (MB) individuals, but that the *acu* mitotype
420 has reduced respiration capacity in the paternal backcross context compared to the *hec* mitotype in
421 the paternal backcross context. In the face of widespread admixture within the hybrid zone,
422 negative selection on the *acu* mitotype might result in the *hec* mitotype increasing in frequency and
423 introgressing westwards. This is indeed what is observed in the wild long-tailed finch hybrid zone,
424 where the centre of the mitochondrial cline is displaced 55 km west of the nuclear cline centre (Fig.
425 1B & C). Respiration capacity reflects the upper limit of mitochondrial aerobic respiration. Therefore,
426 the reduced aerobic capacity observed for *acuticauda* mtDNA paternal backcross individuals is
427 expected to be detrimental, particularly for energetically demanding tissues and life-stages. This
428 suggests that the physiological effects observed in this experiment may be a good proxy for the
429 selection that is occurring in the wild.
430

431 We did not, however, find strong evidence that mitonuclear incompatibilities reduce hybrid
432 fitness compared to parental individuals. There were few differences between our paternal
433 backcross groups and either pure parental individuals or maternal backcross groups (Table 3; Fig. 3B;
434 Fig. S2). A conservative interpretation would suggest that incompatibilities between the
435 mitochondrial and nuclear genomes of these subspecies is not a key component of reproductive
436 isolation between them, which might instead be linked to other incompatibilities such as those
437 involving chromosomal inversions [31]. Our lack of difference between parental and paternal

438 backcross groups are in stark contrast to results from comparable experiments using deeply
439 diverged lineages crossed in the lab (e.g., with mitochondrial divergence >10%), where paternal
440 backcrossed individuals had dramatically impacted mitochondrial function, survival, or fecundity
441 [13,14,62,63]. There are however some lines of evidence suggestive of nascent mitonuclear
442 incompatibility in this study. For a few respiration measures, there was significant or borderline
443 significant differences between paternal backcross and maternal backcross groups; for ETSI,II (Fig.
444 3B) and ETS-II *hec* paternal backcross had higher respiration capacity than did *acu* maternal
445 backcross, and for CxIV the *acu* paternal backcross had borderline significantly lower respiration
446 capacity than *hec* maternal backcross (Table 3; Fig. S2). Furthermore, while not statistically
447 significant, the mean respiration values of both paternal backcross groups were shifted away from
448 the parental groups, which may reflect divergence from the species-specific optima. It is possible
449 that we may simply not have had enough statistical power to detect weak effects. Mitonuclear
450 effects may become more apparent in specific tissue types with high baseline energy demands (e.g.,
451 cardiac or nervous system tissue) or under stressful conditions with heightened energy demands
452 (e.g., during reproduction or thermal stress). Thus, our observations do not rule out a role for
453 mitonuclear incompatibilities creating postzygotic effects on gene flow at this early stage of
454 population divergence.
455
456 We were interested in distinguishing what mitonuclear components were likely interacting
457 to impact mitochondrial aerobic respiration. In particular, we wanted to know whether the observed
458 differences in aerobic respiration between paternal backcross groups was the result of specific
459 protein-protein interactions in complexes I and III or if instead they were due to interactions
460 involving mtDNA encoded tRNA or rRNA. The difference between the two paternal backcross groups
461 was consistent across all measures, which included the CxIV respiration measure that is not
462 dependent on other complexes and there are no fixed differences in CxIV amino acids between
463 subspecies. This suggests that the causal mitonuclear interaction may not be between proteins
464 encoded by the two genomes but may instead be between either mtDNA encoded tRNA and nuDNA
465 encoded aminoacyl tRNA synthetases, or between mtDNA encoded rRNA and nuDNA encoded
466 ribosomal proteins. These interactions would impact the translation of mtDNA and therefore the
467 production of all mtDNA encoded ETS complexes (CxI, III, IV,and V).
468
469 There was also a significant sex difference in the *hecki* subspecies for two measures (OXP-I,II
470 and OXP-I), whereby females had higher respiration capacity than males (Table 3; Fig. S2). As a
471 result, female parental *hecki* individuals had higher respiration capacity than *acuticauda* mtDNA

472 parental backcross individuals, and male parental *hecki* individuals had lower respiration capacity
473 than did *hecki* mtDNA parental backcross individuals. It is unclear to us why there is a sex difference
474 in respiration capacity for *hecki* individuals but not *acuticauda* or backcrossed individuals. This may
475 just be a false positive, as we have run many statistical tests in this study, but it may be biological;
476 sex differences in mitochondrial function have been observed in the literature, although there is no
477 apparent consistent difference[64]. Furthermore, as embryos we would not expect dramatic sex
478 differences in metabolism, except perhaps the gonads. 'Mother's curse' is a phenomenon that can
479 result in a sex effect due to mitonuclear interactions[65–67], but it predicts that detrimental impacts
480 of mtDNA on males and resulting sex differences are exposed with heterospecific nuDNA but not
481 homospecific nuDNA (due to nuDNA coevolution to rescue function), whereas in the present study
482 we found the opposite; that seemingly detrimental impacts of mtDNA only occurs in
483 homo(sub)specific nuDNA context.
484
485 We did not find evidence that the observed effects on cellular aerobic respiration capacity
486 between paternal backcross groups affected our proxies for whole-organism metabolic rate or the
487 level of oxidative damage. The inter-lineage mitonuclear interactions may therefore be impacting
488 fitness through other pathways or under specific circumstances, for example in energetically
489 demanding tissues and life-stages. Given the experimental context it would also be valuable to
490 confirm the whole-body result with more direct measures of metabolism (e.g., open-flow
491 respirometry[68]). This is because other differences between experimental groups may undermine
492 how well heart rate reflects differences in whole-body metabolism, for example at low incubation
493 temperature, Japanese quail heart rate decreases[69] but heart volume increases to compensate (A.
494 Stier, unpublished data).
495
496 Purifying selection appears to be the dominant force in mtDNA evolution in *Poephila* (the
497 mitochondrial genome-wide dN/dS ratio is well below 1 at 0.0168). The observed amino acid
498 differences between long-tailed finch subspecies are thus notable, with all six *hecki*-derived amino
499 acid changes are in genes within complexes I (four AAs) and III (two AAs) and so are candidates for
500 inter-molecular epistasis. In one of the genes with multiple non-synonymous substitutions (COB),
501 amino acid changes were located <15 codon positions apart, potentially indicating some degree of
502 intra-molecular epistasis [57,58]. Taken together this may constitute evidence of adaptive evolution
503 within *hecki*, as mitochondria can contribute to local adaptation (e.g., to differences in climate)[59–
504 61], but to confirm this requires further investigation.
505

In conclusion, we here demonstrate that functional consequences of interactions between mtDNA and nuDNA are possible even at a low level of divergence (<1% mtDNA), and the resulting impact on fitness between the two groups with mitonuclear mismatch in this system may be strong enough to drive mitochondrial introgression across the wild hybrid zone. These mitonuclear interactions may be widespread, as most avian lineages with stable hybrid zones have equal or greater divergence. Researchers considering cases of mitonuclear discordance (or cyto-nuclear discordance more generally) should consider that functional consequences of mitonuclear interactions may be at play[23,70]. Identifying the specific genes involved in mitonuclear interactions in the long-tailed finch would be a valuable direction for future research, as this will facilitate testing the molecular pathways involved in mitonuclear interactions and the evolutionary processes that led to them (e.g., rapid evolution)[20,63,71–74]. This sensitivity of mitochondrial function to genetic variation, their centrality to organismal function (generating 90% of cellular energy in animals[75]), and the broad range of taxa that rely on mitochondria for energy production support suggestions that mitonuclear interactions may be a powerful force acting on hybridising animals[76–79].

## Ethics statement

This experiment was approved by the Macquarie University Animal Ethics Committee (reference number: 2020/021) and all experiments conform to the relevant regulatory standards.

## Funding

This work was supported by an Australian Research Council (ARC) Discovery Project to SCG and DMH (DP180101783), and a Holsworth Wildlife Research Endowment from Equity Trustees Charitable Foundation and the Ecological Society of Australia and a Macquarie University Research Excellence Scholarship to CSM. AS was supported by a 'Turku Collegium for Science and Medicine' Fellowship and a Marie Sklodowska-Curie Postdoctoral Fellowship (#894963). Gerstner Scholars Fellowship and the Gerstner Family Foundation, and the Richard Gilder Graduate School at the American Museum of Natural History provided support to DMH.

## Data and Code Availability Statement

Data from the respiration capacity, oxidative damage, heart rate and mitochondrial copy number, the R scripts for statistical analyses will be uploaded to the Open Science Framework. Mitochondrial sequences for this project will be deposited in GenBank's nucleotide archive. The WGS data used to

assemble mitogenomes is part of another study currently in prep and will be made available when that work is published.

Acknowledgements

The authors would like to thank Riccardo Ton and Hector Pacheco Fuentes for providing assistance setting up the Oroboros $O_2$k, and Macquarie Animal Research Services (M.A.R.S.) staff for providing daily bird husbandry.

Competing interests

The authors declare no competing interests.

Author contributions

Conceptualization, C.S.M., S.C.G.; Methodology, C.S.M., D.M.H., A.S., S.C.G; Investigation, C.S.M.; Data analysis and interpretation, C.S.M., D.M.H., A.S.; Resources, S.C.G.; Writing – Original Draft, C.S.M.; Writing – Review & Editing, C.S.M, D.M.H., A.S., S.C.G.; Visualization, C.S.M., D.M.H.; Supervision, S.C.G.; Funding Acquisition, C.S.M., D.M.H., S.C.G.

## References:

1. Coyne JA, Orr HA. 2004 *Speciation*. Sinauer Associates.

2. Chou J, Leu J. 2010 Speciation through cytonuclear incompatibility: Insights from yeast and implications for higher eukaryotes. *BioEssays* **32**, 401–411. (doi:10.1002/bies.200900162)

3. Bar-Yaacov D, Hadjivasiliou Z, Levin L, Barshad G, Zarivach R, Bouskila A, Mishmar D. 2015 Mitochondrial Involvement in Vertebrate Speciation? The Case of Mito-nuclear Genetic Divergence in Chameleons. *Genome Biology and Evolution* **7**, 3322–3336. (doi:10.1093/gbe/evv226)

4. Hill GE. 2017 The mitonuclear compatibility species concept. *The Auk* **134**, 393–409. (doi:10.1642/auk-16-201.1)

5. Bar-Yaacov D, Blumberg A, Mishmar D. 2012 Mitochondrial-nuclear co-evolution and its effects on OXPHOS activity and regulation. *Biochimica Et Biophysica Acta Bba - Gene Regul Mech* **1819**, 1107–1111. (doi:10.1016/j.bbagrm.2011.10.008)

6. Hill GE. 2020 Mitonuclear Compensatory Coevolution. *Trends in Genetics* **36**, 403–414. (doi:10.1016/j.tig.2020.03.002)

7. Hill. 2019 *Mitonuclear ecology*. Oxford University Press.

573 8. Allio R, Donega S, Galtier N, Nabholz B. 2017 Large Variation in the Ratio of Mitochondrial to
574 Nuclear Mutation Rate across Animals: Implications for Genetic Diversity and the Use of
575 Mitochondrial DNA as a Molecular Marker. *Mol. Biol. Evol.* **34**, 2762–2772.
576 (doi:10.1093/molbev/msx197)

577 9. Willett CS. 2012 Quantifying the Elevation of Mitochondrial DNA Evolutionary Substitution Rates
578 Over Nuclear Rates in the Intertidal Copepod Tigriopus californicus. *J. Mol. Evol.* **74**, 310–318.
579 (doi:10.1007/s00239-012-9508-1)

580 10. Nabholz B, Glémin S, Galtier N. 2008 Strong Variations of Mitochondrial Mutation Rate across
581 Mammals—the Longevity Hypothesis. *Mol. Biol. Evol.* **25**, 120–130. (doi:10.1093/molbev/msm248)

582 11. Nabholz B, Glémin S, Galtier N. 2009 The erratic mitochondrial clock: variations of mutation rate,
583 not population size, affect mtDNA diversity across birds and mammals. *BMC Evol. Biol.* **9**, 54.
584 (doi:10.1186/1471-2148-9-54)

585 12. Mower JP, Touzet P, Gummow JS, Delph LF, Palmer JD. 2007 Extensive variation in synonymous
586 substitution rates in mitochondrial genes of seed plants. *BMC Evol. Biol.* **7**, 135. (doi:10.1186/1471-
587 2148-7-135)

588 13. Ellison CK, Burton RS. 2008 Interpopulation hybrid breakdown maps to the mitochondrial
589 genome. *Evolution* **62**, 631–638. (doi:10.1111/j.1558-5646.2007.00305.x)

590 14. Ellison CK, Niehuis O, Gadau J. 2008 Hybrid breakdown and mitochondrial dysfunction in hybrids
591 of Nasonia parasitoid wasps. *J Evolution Biol* **21**, 1844–1851. (doi:10.1111/j.1420-
592 9101.2008.01608.x)

593 15. Montooth KL, Meiklejohn CD, Abt DN, Rand DM. 2010 Mitochondrial-nuclear epistasis affects
594 fitness within species but does not contribute to fixed incompatibilities between species of
595 Drosophila. *Evolution* **64**, 3364–3379. (doi:10.1111/j.1558-5646.2010.01077.x)

596 16. Arnqvist G, Dowling DK, Eady P, Gay L, Tregenza T, Tuda M, Hosken DJ. 2010 Genetic architecture
597 of metabolic rate: environment specific epistasis between mitochondrial and nuclear genes in an
598 insect. *Evolution* **64**, 3354–3363. (doi:10.1111/j.1558-5646.2010.01135.x)

599 17. Burton RS, Pereira RJ, Barreto FS. 2013 Cytonuclear Genomic Interactions and Hybrid
600 Breakdown. *Annu Rev Ecol Evol Syst* **44**, 281–302. (doi:10.1146/annurev-ecolsys-110512-135758)

601 18. Lee H-Y, Chou J-Y, Cheong L, Chang N-H, Yang S-Y, Leu J-Y. 2008 Incompatibility of Nuclear and
602 Mitochondrial Genomes Causes Hybrid Sterility between Two Yeast Species. *Cell* **135**, 1065–1073.
603 (doi:10.1016/j.cell.2008.10.047)

604 19. Ma H *et al.* 2016 Incompatibility between Nuclear and Mitochondrial Genomes Contributes to an
605 Interspecies Reproductive Barrier. *Cell Metab* **24**, 283–294. (doi:10.1016/j.cmet.2016.06.012)

606 20. Moran B *et al.* 2022 A Lethal Genetic Incompatibility between Naturally Hybridizing Species in
607 Mitochondrial Complex I. , 1–45.

608 21. Toews DPL, Mandic M, Richards JG, Irwin DE. 2014 Migration, mitochondria, and the yellow-
609 rumped warbler. *Evolution* , 1–16. (doi:10.5061/dryad.99db2)

610 22. Morales HE, Pavlova A, Amos N, Major R, Kilian A, Greening C, Sunnucks P. 2018 Concordant
611 divergence of mitogenomes and a mitonuclear gene cluster in bird lineages inhabiting different
612 climates. *Nat Ecol Evol* **2**, 1258–1267. (doi:10.1038/s41559-018-0606-3)

613 23. Wang S, Ore MJ, Mikkelsen EK, Lee-Yaw J, Toews DPL, Rohwer S, Irwin D. 2021 Signatures of
614 mitonuclear coevolution in a warbler species complex. *Nature Communications* **12**, 1–11.
615 (doi:10.1101/2020.04.06.028506)

616 24. Veen T, Borge T, Griffith SC, Saetre G-P, Bures S, Gustafsson L, Sheldon BC. 2001 Hybridization
617 and adaptive mate choice in flycatchers. *Nature* **411**, 45–50. (doi:10.1038/35075000)

618 25. Toews DPL, Brelsford A. 2012 The biogeography of mitochondrial and nuclear discordance in
619 animals. *Mol Ecol* **21**, 3907–3930. (doi:10.1111/j.1365-294x.2012.05664.x)

620 26. Bonnet T, Leblois R, Rousset F, Crochet P-A. 2017 A reassessment of explanations for discordant
621 introgressions of mitochondrial and nuclear genomes. *Evolution* **71**, 2140–2158.
622 (doi:10.1111/evo.13296)

623 27. Hill GE. 2019 Reconciling the Mitonuclear Compatibility Species Concept with Rampant
624 Mitochondrial Introgression. *Integr. Comp. Biol.* **59**, 912–924. (doi:10.1093/icb/icz019)

625 28. Sloan DB, Havird JC, Sharbrough J. 2017 The on-again, off-again relationship between
626 mitochondrial genomes and species boundaries. *Mol. Ecol.* **26**, 2212–2236. (doi:10.1111/mec.13959)

627 29. Stewart JB, Chinnery PF. 2015 The dynamics of mitochondrial DNA heteroplasmy: implications
628 for human health and disease. *Nat Rev Genet* **16**, 530–542. (doi:10.1038/nrg3966)

629 30. Hahn A, Zuryn S. 2019 The Cellular Mitochondrial Genome Landscape in Disease. *Trends Cell Biol*
630 **29**, 227–240. (doi:10.1016/j.tcb.2018.11.004)

631 31. Hooper DM, Griffith SC, Price TD. 2019 Sex chromosome inversions enforce reproductive
632 isolation across an avian hybrid zone. *Mol Ecol* **28**, 1246–1262. (doi:10.1111/mec.14874)

633 32. Lopez KA, McDiarmid CS, Griffith SC, Lovette IJ, Hooper DM. 2021 Evaluating evidence of
634 mitonuclear incompatibilities with the sex chromosomes in an avian hybrid zone. *Evolution* **75**,
635 1395–1414. (doi:10.1111/evo.14243)

636 33. Koch RE *et al.* 2021 Integrating Mitochondrial Aerobic Metabolism into Ecology and Evolution.
637 *Trends Ecol Evol* **36**, 321–332. (doi:10.1016/j.tree.2020.12.006)

638 34. Brazill-Boast J, van Rooij EP, Pryke SR, Griffith SC. 2011 Interference from long-tailed finches
639 constrains reproduction in the endangered Gouldian finch. *J Anim Ecol* **80**, 39–48.

640 35. Rowe M, Griffith SC, Hofgaard A, Lifjeld JT. 2015 Subspecific variation in sperm morphology and
641 performance in the Long-tailed Finch (Poephila acuticauda). *Avian Research* , 1–10.
642 (doi:10.1186/s40657-015-0032-z)

643 36. Singhal S, Leffer EM, Sannareddy K, Turner I, Venn O, Hooper DM, Strand AI. 2015 Stable
644 recombination hotspots in birds. *Science* , 1–6.

645 37. Sheldon EL, McCowan LSC, McDiarmid CS, Griffith SC. 2018 Measuring the embryonic heart rate
646 of wild birds: An opportunity to take the pulse on early development. *The Auk* **135**, 71–82.
647 (doi:10.1642/auk-17-111.1)

648 38. Martindale JL, Holbrook NJ. 2002 Cellular response to oxidative stress: Signaling for suicide and
649 survival*. *J. Cell. Physiol.* **192**, 1–15. (doi:10.1002/jcp.10119)

650 39. Birben E, Sahiner UM, Sackesen C, Erzurum S, Kalayci O. 2012 Oxidative Stress and Antioxidant
651 Defense. *World Allergy Organization J* **5**, 9–19. (doi:10.1097/wox.0b013e3182439613)

652 40. Marasco V, Stier A, Boner W, Griffiths K, Heidinger B, Monaghan P. 2017 Environmental
653 conditions can modulate the links among oxidative stress, age, and longevity. *Mech Ageing Dev* **164**,
654 100–107. (doi:10.1016/j.mad.2017.04.012)

655 41. Stier A, Romestaing C, Schull Q, Lefol E, Robin J, Roussel D, Bize P. 2017 How to measure
656 mitochondrial function in birds using red blood cells: a case study in the king penguin and
657 perspectives in ecology and evolution. *Methods Ecol Evol* **8**, 1172–1182. (doi:10.1111/2041-
658 210x.12724)

659 42. Ton R, Stier A, Cooper CE, Griffith SC. 2021 Effects of Heat Waves During Post-natal Development
660 on Mitochondrial and Whole Body Physiology: An Experimental Study in Zebra Finches. *Front Physiol*
661 **12**, 661670. (doi:10.3389/fphys.2021.661670)

662 43. Lee JC-I *et al.* 2010 A novel strategy for avian species and gender identification using the CHD
663 gene. *Mol Cell Probe* **24**, 27–31. (doi:10.1016/j.mcp.2009.08.003)

664 44. Sorenson MD, Quinn TW. 1998 Numts: A Challenge for Avian Systematics and Population
665 Biology. *Auk* **115**, 214–221. (doi:10.2307/4089130)

666 45. Valavanidis A, Vlachogianni T, FIOTAKIS C. 2009 8-hydroxy-2' -deoxyguanosine (8-OHdG): A
667 Critical Biomarker of Oxidative Stress and Carcinogenesis. *J Environ Sci Heal Part C* **27**, 120–139.
668 (doi:10.1080/10590500902885684)

669 46. Stier A, Schull Q, Bize P, Lefol E, Haussmann M, Roussel D, Robin J-P, Viblanc VA. 2019 Oxidative
670 stress and mitochondrial responses to stress exposure suggest that king penguins are naturally
671 equipped to resist stress. *Sci Rep-uk* **9**, 8545. (doi:10.1038/s41598-019-44990-x)

672 47. Stier A, Monaghan P, Metcalfe NB. 2022 Experimental demonstration of prenatal programming
673 of mitochondrial aerobic metabolism lasting until adulthood. *Proc Royal Soc B* **289**, 20212679.
674 (doi:10.1098/rspb.2021.2679)

675 48. Meiklejohn CD, Holmbeck MA, Siddiq MA, Abt DN, Rand DM, Montooth KL. 2013 An
676 Incompatibility between a Mitochondrial tRNA and Its Nuclear-Encoded tRNA Synthetase
677 Compromises Development and Fitness in Drosophila. *Plos Genet* **9**, e1003238.
678 (doi:10.1371/journal.pgen.1003238)

679 49. Li H. 2011 A statistical framework for SNP calling, mutation discovery, association mapping and
680 population genetical parameter estimation from sequencing data. *Bioinformatics* **27**, 2987–2993.
681 (doi:10.1093/bioinformatics/btr509)

682 50. Donath A, Jühling F, Al-Arab M, Bernhart SH, Reinhardt F, Stadler PF, Middendorf M, Bernt M.
683 2019 Improved annotation of protein-coding genes boundaries in metazoan mitochondrial genomes.
684 *Nucleic Acids Res* **47**, 10543–10552. (doi:10.1093/nar/gkz833)

685 51. Katoh K, Rozewicki J, Yamada KD. 2017 MAFFT online service: multiple sequence alignment,
686 interactive sequence choice and visualization. *Brief. Bioinform.* **20**, bbx108-.
687 (doi:10.1093/bib/bbx108)

688 52. Gao F, Chen C, Arab DA, Du Z, He Y, Ho SYW. 2019 EasyCodeML: A visual tool for analysis of
689 selection using CodeML. *Ecol. Evol.* **9**, 3891–3898. (doi:10.1002/ece3.5015)

690 53. Bates D, Mächler M, Bolker B, Walker S. 2015 Fitting Linear Mixed-Effects Models Using lme4. *J.*
691 *Stat. Soft.* **67**, 1-47\8. (doi:10.18637/jss.v067.i01)

692 54. Kuznetsova A, Brockhoff P, Christensen R. 2017 lmerTest Package: Tests in Linear Mixed Effects
693 Models. *Journal of Statistical Software* **82**, 1–26. (doi:10.18637/jss.v082.i13)

694 55. Lenth R. 2020 emmeans: Estimated Maringal Means, aka Least-Squares Means. R package.

695 56. Hartig F. 2021 Residual Diagnostics for Hierarchical (Multi-Level / Mixed) Regression Models [R
696 package DHARMa version 0.4.4].

697 57. Callahan B, Neher RA, Bachtrog D, Andolfatto P, Shraiman BI. 2011 Correlated Evolution of
698 Nearby Residues in Drosophilid Proteins. *Plos Genet* **7**, e1001315.
699 (doi:10.1371/journal.pgen.1001315)

700 58. Storz JF. 2018 Compensatory mutations and epistasis for protein function. *Curr Opin Struc Biol*
701 **50**, 18–25. (doi:10.1016/j.sbi.2017.10.009)

702 59. Lajbner Z, Pnini R, Camus MF, Miller J, Dowling DK. 2018 Experimental evidence that thermal
703 selection shapes mitochondrial genome evolution. *Sci Rep-uk* **8**, 9500. (doi:10.1038/s41598-018-
704 27805-3)

705 60. Lamb AM, Gan HM, Greening C, Joseph L, Lee YP, Morán-Ordóñez A, Sunnucks P, Pavlova A. 2018
706 Climate-driven mitochondrial selection: A test in Australian songbirds. *Mol Ecol* **27**, 898–918.
707 (doi:10.1111/mec.14488)

708 61. Lasne C, Heerwaarden B, Sgrò CM, Connallon T. 2019 Quantifying the relative contributions of
709 the X chromosome, autosomes, and mitochondrial genome to local adaptation*. *Evolution* **73**, 262–
710 277. (doi:10.1111/evo.13647)

711 62. Barreto FS, Burton RS. 2013 Elevated oxidative damage is correlated with reduced fitness in
712 interpopulation hybrids of a marine copepod. *Proc. R. Soc. B* **280**, 20131521–20131521.
713 (doi:10.1098/rspb.2013.1521)

714 63. Barreto FS, Watson ET, Lima TG, Willett CS, Edmands S, Li W, Burton RS. 2018 Genomic
715 signatures of mitonuclear coevolution across populations of Tigriopus californicus. *Nat Ecol Evol* **2**,
716 1250–1257. (doi:10.1038/s41559-018-0588-1)

717 64. Junker A *et al.* 2022 Human studies of mitochondrial biology demonstrate an overall lack of
718 binary sex differences: A multivariate meta-analysis. *Faseb J* **36**, e22146.
719 (doi:10.1096/fj.202101628r)

720 65. Dowling DK, Adrian RE. 2019 Challenges and Prospects for Testing the Mother's Curse
721 Hypothesis. *Integr Comp Biol* **59**, 875–889. (doi:10.1093/icb/icz110)

722 66. Carnegie L, Reuter M, Fowler K, Lane N, Camus MF. 2021 Mother's curse is pervasive across a
723 large mitonuclear Drosophila panel. *Evol Lett* **5**, 230–239. (doi:10.1002/evl3.221)

724 67. Nagarajan-Radha V, Aitkenhead I, Clancy DJ, Chown SL, Dowling DK. 2020 Sex-specific effects of
725 mitochondrial haplotype on metabolic rate in Drosophila melanogaster support predictions of the
726 Mother's Curse hypothesis. *Philosophical Transactions Royal Soc B* **375**, 20190178.
727 (doi:10.1098/rstb.2019.0178)

728 68. Cooper CE, Hurley LL, Griffith SC. 2020 Effect of acute exposure to high ambient temperature on
729 the thermal, metabolic and hygric physiology of a small desert bird. *Comp Biochem Physiology Part*
730 *Mol Integr Physiology* **244**, 110684. (doi:10.1016/j.cbpa.2020.110684)

731 69. Stier A, Metcalfe NB, Monaghan P. 2020 Pace and stability of embryonic development affect
732 telomere dynamics: an experimental study in a precocial bird model. *Proc Royal Soc B* **287**,
733 20201378. (doi:10.1098/rspb.2020.1378)

734 70. Nikelski E, Rubtsov AS, Irwin D. 2022 High heterogeneity in genomic differentiation between
735 phenotypically divergent songbirds: a test of mitonuclear co-introgression. *Heredity* , 1–13.
736 (doi:10.1038/s41437-022-00580-8)

737 71. Baris TZ, Wagner DN, Dayan DI, Du X, Blier PU, Pichaud N, Oleksiak MF, Crawford DL. 2017
738 Evolved genetic and phenotypic differences due to mitochondrial-nuclear interactions. *Plos Genet*
739 **13**, e1006517. (doi:10.1371/journal.pgen.1006517)

740 72. Nguyen THM *et al.* 2022 Mapping mitonuclear epistasis using a novel recombinant yeast
741 population. *Biorxiv* , 2022.08.31.505974. (doi:10.1101/2022.08.31.505974)

742 73. Healy TM, Burton RS. 2022 Differential gene expression and mitonuclear incompatibilities in fast-
743 and slow-developing inter-population Tigriopus californicus hybrids. *Biorxiv* , 2022.09.09.507197.
744 (doi:10.1101/2022.09.09.507197)

745 74. Healy TM, Burton RS. 2022 Genetic incompatibilities in reciprocal hybrids between populations
746 of Tigriopus californicus with low to moderate mitochondrial sequence divergence. *Biorxiv* ,
747 2022.09.19.508600. (doi:10.1101/2022.09.19.508600)

748 75. Harris DA, Das AM. 1991 Control of mitochondrial ATP synthesis in the heart. *Biochem J* **280**,
749 561–573. (doi:10.1042/bj2800561)

750 76. Wolff JN, Ladoukakis ED, Enriquez JA, Dowling DK. 2014 Mitonuclear interactions: evolutionary
751 consequences over multiple biological scales. *Philosophical Transactions of the Royal Society B:*
752 *Biological Sciences* **369**, 20130443–20130443. (doi:10.1098/rstb.2013.0443)

753 77. Hill GE. 2016 Mitonuclear coevolution as the genesis of speciation and the mitochondrial DNA
754 barcode gap. *Ecol Evol* **6**, 5831–5842. (doi:10.1002/ece3.2338)

755 78. Hill GE, Havird JC, Sloan DB, Burton RS, Greening C, Dowling DK. 2019 Assessing the fitness
756 consequences of mitonuclear interactions in natural populations. *Biol Rev* **94**, 1089–1104.
757 (doi:10.1111/brv.12493)

758 79. Pereira RJ, Lima TG, Pierce-Ward NT, Chao L, Burton RS. 2021 Recovery from hybrid breakdown
759 reveals a complex genetic architecture of mitonuclear incompatibilities. *Mol Ecol* **30**, 6403–6416.
760 (doi:10.1111/mec.15985)

761

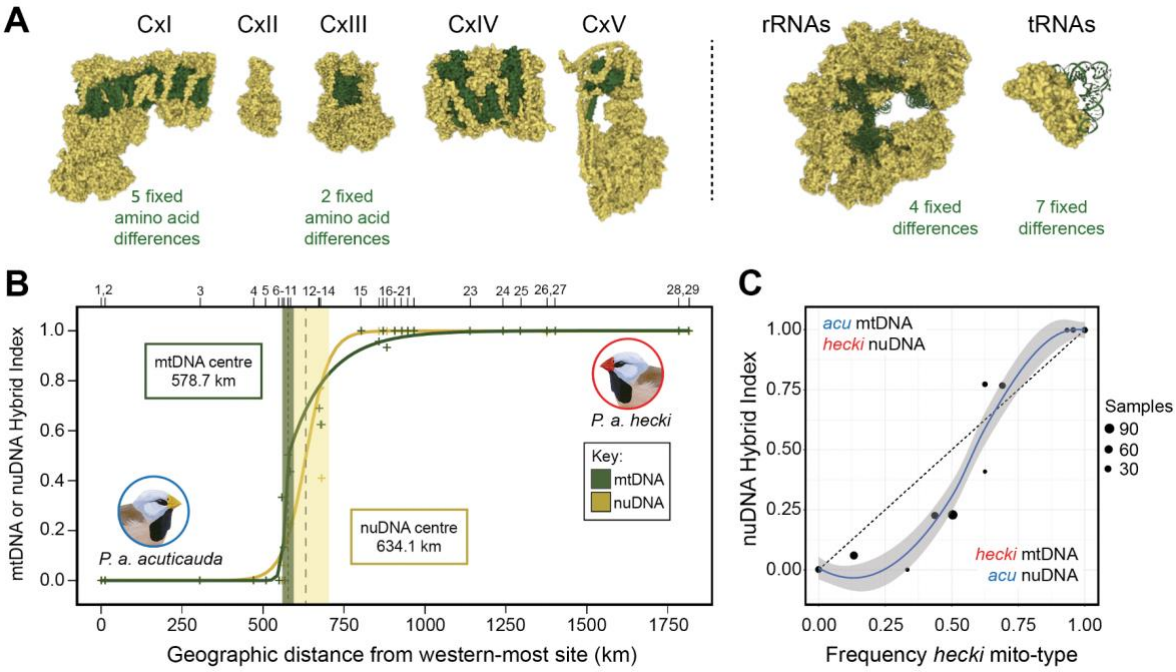


**Figure 1 | Mitochondrial and nuclear genes in the long-tailed finch. (A)** Key components of mitochondria that are encoded by both the mitochondrial (green) and nuclear (yellow) genomes. This includes proteins that form the electron transport system complexes (CxI-IV) and ATP synthase (CxV), as well as mitochondrial ribosomes and transfer RNA-tRNA sythetase. Note that complexes are not to scale. The animals and PBD accession numbers for each are CxI (bovine, 5LNK), CxII (chicken, 2H89), CxIII (chicken, 3CWB), CxIV (bovine, 1V45), CxV (bovine, 5ARA – TBC), tRNA (yeast, 4YYE), rRNA (humans, 3J9M). Figure inspired by Hill et al. 2019. **(B)** Geographic clines for mtDNA and nuDNA (Z-chromosome) across the distribution of the long-tailed finch, with the mtDNA cline centre 55 km to the west of nuDNA cline centre. Locations of the 29 sampled populations are given above the panel and population means for mtDNA and nuDNA given as green or yellow crosses, respectively. **(C)** The frequency of the hecki mito-type against hybrid index for each of the 29 sampled hybrid zone populations, with a loess curve with 95% CI fitted to the data against a dashed line showing the 1:1 neutral expectation. (B) and (C) are based on re-evaluated and re-plotted published data from Lopez et al. 2021.

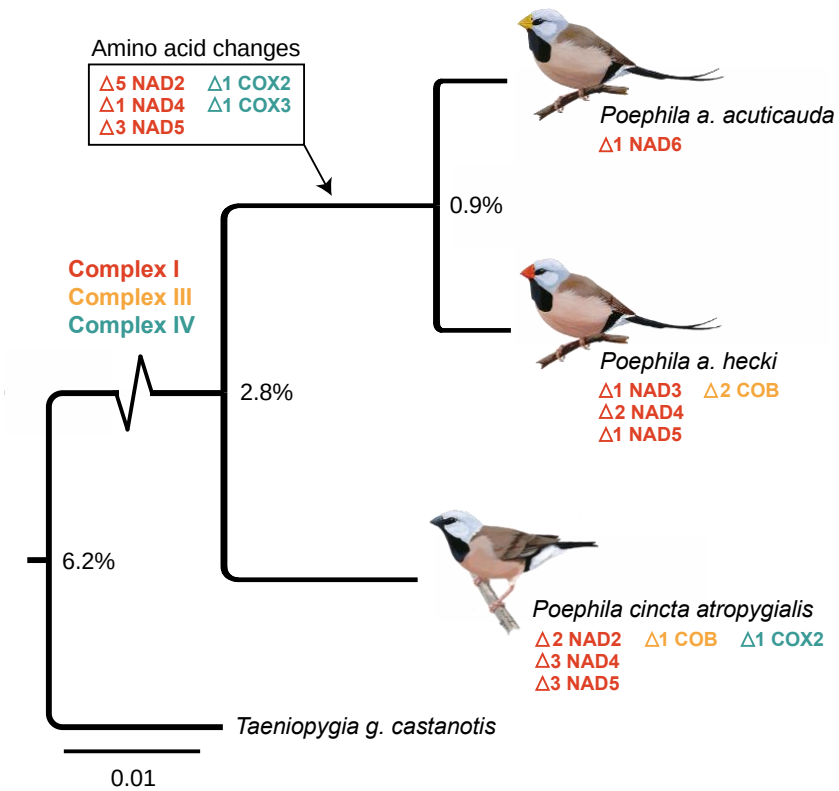


**Figure 2 | Maximum likelihood mtDNA phylogeny, net divergence in protein-coding genes, and inferred lineage of origin for all amino acid changes identified between long-tailed finch subspecies and the black-throated finch.** Maximum likelihood trees were generated based on an aligned concatenation of consensus sequences for all 13 protein-coding genes using W-IQ-TREE [1] under the identified the best-fit substitution model: TPM2u+F+I. The zebra finch (NCBI accession: DQ422742) and black-throated finch samples were used to polarize all nucleotide substitutions and any associated amino acid changes to their branch of origin. Branch lengths are proportional to the number of substitutions in the coding regions. Divergence estimates at each node represent the total number of fixed differences between species in protein-coding genes divided by the total number of protein-coding bases (Table S2). The number of amino acid changes identified within each gene are color-coded based on their associated ETS complex: red for complex I, yellow for complex III, and blue-green for complex IV.

A

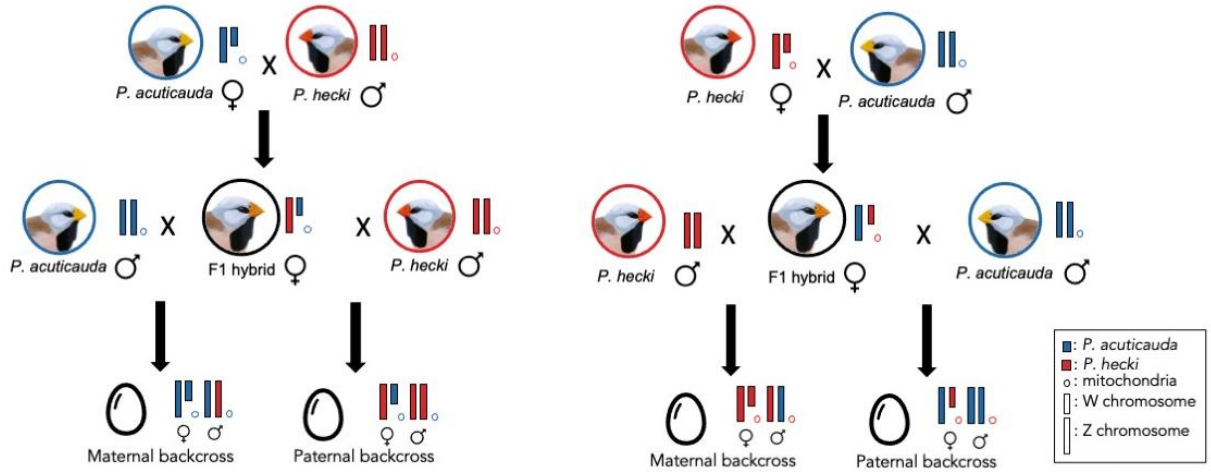


B

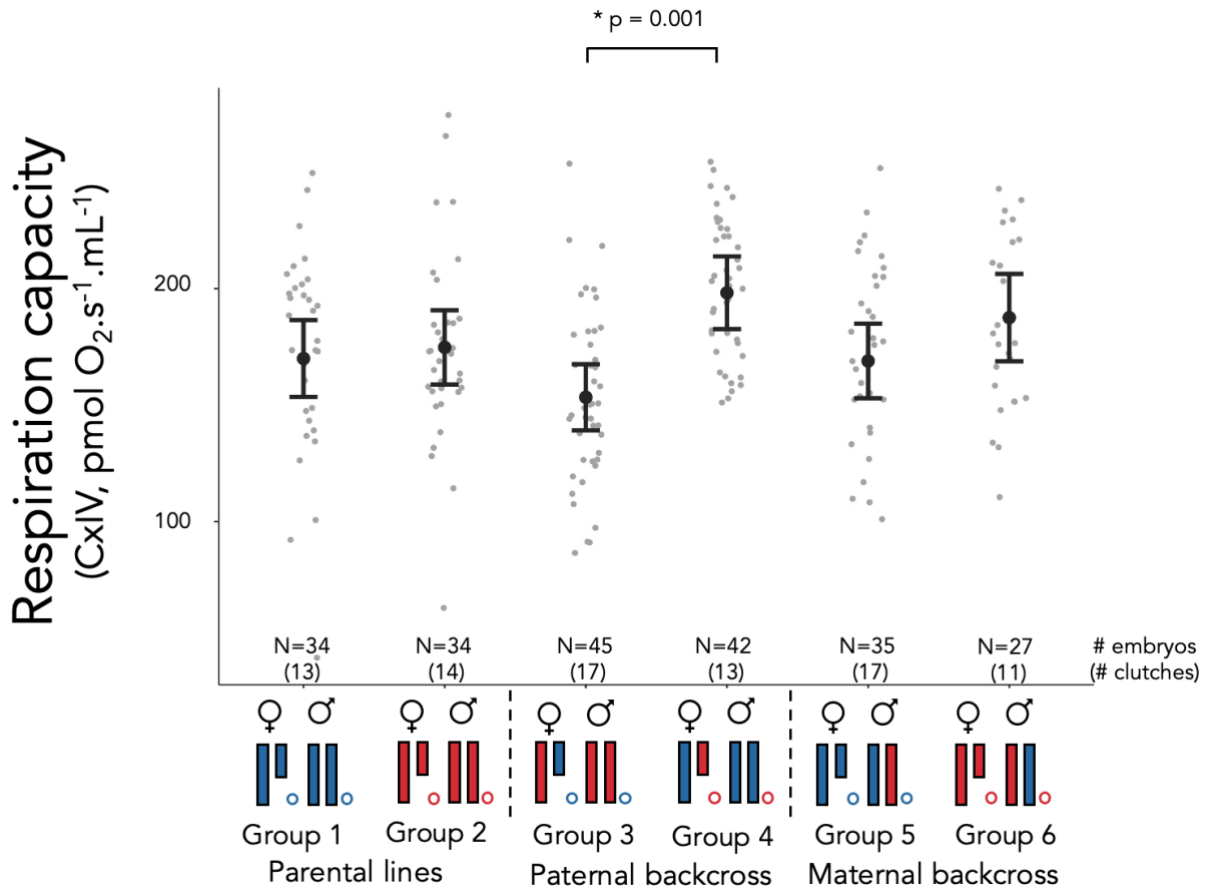


**Figure 3 | Mitochondrial and nuclear genomes between the long-tailed finch subspecies interact to impact mitochondrial respiration capacity. (A)** The crossing design employed to generate paternal and maternal backcross offspring. **(B)** The respiration capacity of our experimental groups, with grey datapoints indicating raw data (corrected for amount of protein), and black mean and 95% CIs reflect model output (accounting for clutch ID, protein

quantity, length of time in chamber, sex). Most measures of mitochondrial respiration capacity had this same pattern of differences among the groups (Table 2; Supp Fig 2).

**References**

1. Trifinopoulos J, Nguyen L-T, von Haeseler A, Minh BQ. 2016 W-IQ-TREE: a fast online phylogenetic tool for maximum likelihood analysis. Nucleic Acids Res. 44, W232–W235. (doi:10.1093/nar/gkw256)

**Table 1** | Mitochondrial protein-coding divergence between long-tailed finch subspecies. The 13 protein-coding genes comprising the electron transport system (ETS) are organized by complex. Fixed differences between subspecies were inferred based on comparison of full mitochondrial genomes of *Poephila a. acuticauda* (N = 14) and *P. a. hecki* (N = 11) with $D_{XY}$ calculated as the absolute divergence between members of each subspecies. Estimates of dN/dS, ratio of the rate of non-synonymous to the rate of synonymous nucleotide substitutions, were calculated for each gene using the model M0 implemented in the program Easy-CodeML (v1.41; Gao et al 2019). The combined estimate of dN/dS was inferred based on net dN (0.0114) and dS (0.6802) across all protein-coding genes.

| Complex | Gene | Fixed differences | $D_{XY}$ | dN/dS |
|---|---|---|---|---|
| Complex I | *NAD1* | 12 | 0.012 | 0.0001 |
| | *NAD2* | 8 | 0.008 | 0.0001 |
| | *NAD3* | 3 | 0.009 | 0.1142 |
| | *NAD4* | 9 | 0.007 | 0.0599 |
| | *NAD4L* | 5 | 0.017 | 0.0001 |
| | *NAD5* | 17 | 0.009 | 0.0127 |
| | *NAD6* | 17 | 0.033 | 0.0210 |
| Complex III | *COB* | 10 | 0.009 | 0.0574 |
| Complex IV | *COX1* | 9 | 0.006 | 0.0001 |
| | *COX2* | 4 | 0.006 | 0.0001 |
| | *COX3* | 3 | 0.004 | 0.0001 |
| Complex V | *ATP6* | 10 | 0.015 | 0.0001 |
| | *ATP8* | 0 | 0.000 | 0.0001 |
| | **Combined** | **107** | **0.009** | **0.0168** |

**Table 2 |** Summary of mtDNA amino acid differences between long-tailed finch subspecies in protein-coding genes of the ETS. Fixed differences between subspecies were assigned (i.e., polarized) to their lineage of origin using mitochondrial genomes of the black-throated finch (*Poephila cincta atropygialis*; N = 11), sister species to the long-tailed finch, and the zebra finch (*Taeniopygia guttata*; N = 1). Mutation notation represents the ancestral amino acid, it's position in the gene, and the derive amino acid (e.g., mutation T9A represents an amino acid change from a Threonine [T] to an Alanine [A] at amino acid position nine). The biochemical property differences associated with a change in amino acid are noted.

| Complex | Gene | Mutation | Biochemical Change | Origin |
|---|---|---|---|---|
| Complex I | *NAD3* | T9A | polarity change (+ > -) | *hecki* |
| | *NAD4* | T96A | polarity change (+ > -) | *hecki* |
| | *NAD4* | T398A | polarity change (+ > -) | *hecki* |
| | *NAD5* | A16V | none | *hecki* |
| | *NAD6* | S127L | polarity change (+ > -) | *acuticauda* |
| Complex III | *COB* | S358T | none | *hecki* |
| | *COB* | I372M | none | *hecki* |

**Table 3 |** Model output comparing the measures of mitochondrial function and physiology measures among the six experimental groups.

| **Respiration measure** | ETS Cxs included | Description of measure | Repeatability (SE) from 40 samples run in duplicate | Cross*Sex<br>X2 (DF) p-value | Sex (if split model due to interaction) | Cross<br>X2 (DF) p-value | Sex<br>X2 (DF) p-value | Protein Qty<br>X2 (DF) p-value | Length of time<br>X2 (DF) p-value | Var. | Marg $R^2$ | ICC Pair ID | Cond $R^2$ | G3<G4 | G4>G5 | G2<G4 | G2>G3 | G3<G6 |
|---|---|---|---|---|---|---|---|---|---|---|---|---|---|---|---|---|---|---|
| | | | | | | | | | | | | | | Showing p-values for p < 0.1. | | | | |
| OXP-I,II | I,II,III,IV,V | Coupled respiration | 0.94 (0.02) | **11.5 (5) 0.043** | Female | **12.73 (5) 0.026** | NA | 2.59 (1) 0.11 | **8.68 (1) 0.003** | 197 | 0.62 | 0.37 | 0.99 | *0.064* | | | *0.072* | |
| | | | | | Male | **13.87 (5) 0.016** | NA | **7.98 (1) 0.005** | **9.31 (1) 0.002** | 240 | 0.44 | 0.55 | 0.99 | **0.042** | | *0.093* | | |
| ETS-I,II | I,II,III,IV | Uncoupled respiration | 0.90 (0.03) | 9.78 (5) 0.08 | | **20.15 (5) 0.001** | 2.3 (1) 0.13 | **4.06 (1) 0.044** | **26.1 (1) <0.001** | 289 | 0.53 | 0.46 | 0.99 | **<0.001** | **0.034** | | | |
| OXP-I | I,III,IV,V | Coupled respiration | 0.69 (0.09) | **11.97 (5) 0.035** | Female | **15.4 (5) 0.009** | NA | *3.29 (1) 0.07* | **25.2 (1) <0.001** | 206 | 0.79 | 0.20 | 0.99 | **0.029** | | | **0.036** | |
| | | | | | Male | **14.9 (5) 0.010** | NA | **6.67 (1) 0.010** | **33.11 (1) <0.001** | 224 | 0.63 | 0.36 | 0.99 | **0.030** | | *0.052* | | |
| ETS-II | II,III,IV | Maximum capacity of the ETS | 0.96 (0.01) | 7.1 (5) 0.2 | | **19.6 (5) 0.002** | 1.53 (1) 0.22 | **5.04 (1) 0.02** | 1.17 (1) 0.28 | 55 | 0.39 | 0.58 | 0.98 | **0.001** | *0.065* | | | |
| CxIV | IV | Maximum respiration | 0.93 (0.02) | 8.7 (5) 0.12 | | **19.8 (5) 0.001** | 1.5 (1) 0.22 | **7.8 (1) 0.005** | 2.14 (1) 0.14 | 302 | 0.41 | 0.58 | 0.99 | **0.001** | | | | *0.056* |
| LEAK-I,II | I,II,III,IV | Respiration linked to proton leak | 0.89 (0.03) | *9.6 (5) 0.09* | | **17.3 (5) 0.004** | 2.4 (1) 0.12 | **8.6 (1) 0.003** | 0.3 (1) 0.58 | 1.4 | 0.19 | 0.36 | 0.55 | **0.003** | | | | |
| | | | | | | | | | | | | | | | | | | |
| **Measure** | | | | Cross*Sex | Sex (if split model due to interaction) | Cross | Sex | Embryo Mass | | Var. | Marg $R^2$ | ICC Pair ID | Cond $R^2$ | | | | | |
| Embryo Mass | | | | 8.6 (5) 0.13 | | 7.3 (5) 0.20 | 0.01 (1) 0.92 | NA | | <0.001 | <0.001 | <0.001 | <0.001 | | | | | |
| Embryo Survival | | | | NA | | 4.1 (5) 0.53 | NA | NA | | 0.09 | 0.02 | 0.24 | 0.27 | | | | | |
| Heart rate (proxy for whole body metabolism) | | | | 15.2 (5) 0.01 | Male | 7.8 (5) 0.17 | NA | **23.5 (1) <0.01** | | 156 | 0.41 | 0.59 | 0.99 | | | | | |
| | | | | | Female | 6.3 (5) 0.28 | NA | **8.3 (1) 0.004** | | 78 | 0.20 | 0.80 | 0.99 | | | | | |
| Oxidative DNA oxidative damage (log transformed) | | | | 8.3 (5) 0.14 | | 8.6 (5) 0.12 | *3.0 (1) 0.08* | NA | ICC Plate: 0.008 | 0.019 | 0.006 | 0.012 | 0.026 | | | | | |
| mtDNA copy number (log transformed) | | | | 2.2 (5) 0.82 | | **20.9 (5) <0.001** | 0.17 (1) 0.69 | NA | ICC Plate: 0.00 | 0.03 | 0.01 | 0.02 | 0.03 | G5<G6 **0.005** | G1<G6 *0.093* | G3<G6 *0.090* | | |

Groups same as that in Figure 2. Group 1; parental group *acuticauda*, Group 2: parental group *hecki*, Group 3: paternal backcross *acuticauda* mitotype, Group 4: paternal backcross *hecki* mitotype, Group 5: maternal backcross *acuticauda* mitotype, Group 6: maternal backcross *hecki* mitotype.

Var. - variance, Marg$R^2$ – marginal $R^2$ , ICC Pair ID – intra-class correlation coefficient value for Pair ID as a random effect, CondR2 – conditional $R^2$.